HMGN2 induces pyroptosis in tumour cells by modulating the STT3B/PD-L1/caspase-1/GSDMD axis

WENWEN HAN, HONGLI CHEN, BOMIAO CUI, JIAO CHEN, PING ZHANG and YUN FENG

State Key Laboratory of Oral Diseases and National Clinical Research Centre for Oral Diseases and West China Hospital of Stomatology, Sichuan University, Chengdu, Sichuan 610041, P.R. China

Received August 25, 2025; Accepted November 26, 2025

DOI: 10.3892/mmr.2026.13807

Abstract. High-mobility group nucleosomal-binding domain 2 (HMGN2) is an abundant conserved protein that acts as a non-histone nuclear DNA-binding protein. HMGN2 can be released by activated peripheral blood mononuclear cells, $CD8^+$ T cells and γδ T cells, and can induce tumour cell apoptosis. In the present study, receptors of HMGN2 were detected on tumour cell membranes and the mechanism by which HMGN2 induces tumour cell apoptosis was examined. Flow cytometry was used to determine the degree of HMGN2-induced apoptosis. To identify notable HMGN2 receptors on tumour cells, the present study used immunoprecipitation and mass spectrometry (IP/MS) to identify protein complexes. Western blotting and immunofluorescence were used to confirm interactions between HMGN2 and oligosaccharyltransferase subunit STT3B (STT3B), and to elucidate the downstream regulatory mechanism of HMGN2. The predictive tools ZDOCK and AlphaFold3 were used to determine the binding conformation of HMGN2 to STT3B. HMGN2 was shown to bind to the membrane and induce the apoptosis of CAL-27 tumour cells. STT3B was identified via IP/MS as a receptor of HMGN2 on the CAL-27 membrane and subsequently identified as an important receptor of HMGN2 via an anti-STT3B blocking assay. ZDOCK and AlphaFold3 analyses revealed that HMGN2 and STT3B formed a stable protein docking model. After incubation with HMGN2, the expression of programmed cell death 1 ligand 1 (PD-L1)/caspase-1/gasdermin D (GSDMD) axis components was significantly increased, and PD-L1 was translocated into the nucleus from the membrane of CAL-27 cells. The results of the present study indicated that extracellular HMGN2 induced pyroptosis in tumour cells by modulating the STT3B/PD-L1/caspase-1/GSDMD axis.

Correspondence to: Professor Yun Feng or Professor Ping Zhang, State Key Laboratory of Oral Diseases and National Clinical Research Centre for Oral Diseases and West China Hospital of Stomatology, Sichuan University, 14 Renmin South Road, Chengdu, Sichuan 610041, P.R. China
E-mail: 953463551@qq.com
E-mail: pingzhang68@hotmail.com

Key words: high-mobility group nucleosomal-binding domain 2, oligosaccharyltransferase subunit STT3B, programmed cell death 1 ligand 1, pyroptosis, antitumour effect

Introduction

High-mobility group (HMG) nucleosomal-binding domain 2 (HMGN2) is an abundant conserved protein that acts as a non-histone nuclear DNA-binding protein. Studies have suggested that HMGN2 interacts with transcription factors and chromatin, leading to the modulation of gene transcription (1-4). A previous study revealed that the HMGN2 protein is secreted by activated peripheral blood mononuclear cells, $CD8^+$ T cells and γδ T cells, where it induces tumour cell apoptosis (5,6). However, the precise mechanism of action of HMGN2 remains to be elucidated. Cytolytic T lymphocytes (CTLs) are key antitumour immune cells that are rich in cytoplasmic granules. Upon degranulation, CTLs secrete cytotoxic molecules, such as TNF-α, IFN-γ and IL-2, against target cells (7). Cytoplasmic granules in CTLs contain perforin, granzymes, granulysin and other effector molecules involved in the antitumour response (8,9).

A study by Li *et al* (10) reported that the N-terminal structure of HMGN2 can recognize and adhere to tumour cells. In addition, Fan *et al* (11) revealed that HMGN2 can modulate DNA transcription and translation, thus inducing tumour cell apoptosis. Despite these findings, the detailed mechanism by which HMGN2 affects tumour cells remains to be elucidated.

The oligosaccharyltransferase (OST) subunit STT3 (STT3) protein is an important enzyme of the OST complex, which consists of two isoforms in mammalian cells: STT3A and STT3B. As the catalytic subunits of the OST complex, STT3 isoforms can initiate N-glycosylation by catalysing the transfer of a 14-sugar core glycan from dolichol to the asparagine residues of substrates (12). Evidence indicates that the expression of STT3 isoforms, including STT3A and STT3B, which are upregulated during epithelial-mesenchymal transition (EMT), is important for the glycosylation and stabilization of programmed cell death 1 ligand 1 (PD-L1), thus facilitating immune evasion in tumour cells (13).

The present study aimed to identify the receptors of HMGN2 on tumour cell membranes and to investigate the underlying mechanisms of HMGN2 in human tongue squamous carcinoma CAL-27 cells.

Materials and methods

Cell culture. The human tongue squamous cell carcinoma cell line CAL-27 was obtained from the Biobank of West China Hospital of Stomatology Sichuan University (Chengdu, China). The cells were cultured in DMEM (cat. no. 10-013-CVRC; Corning, Inc.) supplemented with 10% foetal bovine serum (cat. no. A5256701; Gibco; Thermo Fisher Scientific, Inc.) in a cell culture dish at 37˚C in a humidified atmosphere containing 5% CO_2.

Effect of HMGN2 on CAL-27 cells. Recombinant HMGN2 with an N-terminal His-tag expressed in *Escherichia coli* and purified to >90% purity (cat. no. RPB057Hu01) was purchased from CLOUD-CLONE CORP., and diluted with PBS.

A total of ~1x10^5 CAL-27 cells were seeded and cultured in 12-well plates until sub-confluent, after which His-tagged HMGN2 (0, 5, 10 and 20 μg/ml) was added and the cells were incubated at 37˚C for 24 h. The control group was treated with PBS. After the cells were washed with 1X PBS, a FLUOVIEW FV3000 bright-field microscope (Olympus Corporation) was used to observe the cellular state and images were captured.

A total of 20 μg/ml fluorescein isothiocyanate (FITC)-labelled HMGN2 was added for incubation with CAL-27 cells at 37˚C for 10 min, 1 and 2 h, as described in a previous study (5). Nuclear staining of CAL-27 cells was performed using Hoechst 33258 (cat. no. A3466; APExBIO Technology LLC) at room temperature for 10 min. After the cells were washed with 1X PBS, a FLUOVIEW FV3000 confocal laser scanning microscope (Olympus Corporation) was used to observe the cellular state and images were captured.

Apoptosis analysis. An Annexin V-FITC apoptosis detection kit (cat. no. K2003; APExBIO Technology LLC) was used to detect apoptosis according to the manufacturer's instructions. A total of ~1x10^5 CAL-27 cells were seeded and cultured in 12-well plates until sub-confluent, after which His-tagged HMGN2 (20 μg/ml) was added for incubation at 37˚C for 12 or 24 h. The cells were then washed with 1X PBS and resuspended in 500 μl 1X binding buffer (cat. no. K2003; APExBIO Technology LLC). Subsequently, 5 μl Annexin V-FITC and 5 μl PI were added, and the samples were incubated in the dark at room temperature for 20 min. A CytoFLEX flow cytometer (Beckman Coulter, Inc.) was used for apoptosis analysis. The flow cytometry data were analyzed using Kaluza Analysis software (version 2.4.0; Beckman Coulter, Inc.).

Immunoprecipitation and mass spectrometry (IP/MS). After washing with 1X PBS, ~1x10^7 CAL-27 cells cultured in 100-mm culture dishes were incubated with 20 μg/ml His-tagged HMGN2 at 37˚C for 60 min. Cells were harvested by scraping in 1X PBS, and membrane proteins were isolated using a commercial membrane protein extraction kit (cat. no. EX1110; Beijing Solarbio Science & Technology Co., Ltd.) with the following steps: The cells were centrifuged at 500 x g for 5 min at 4˚C, washed twice with 1X PBS, and resuspended in chilled Membrane Protein Extraction Buffer A. The suspension was shaken at 4˚C for 30 min, followed by centrifugation at 12,000 x g for 5 min at 4˚C. The supernatant was collected, incubated in a 37˚C water bath for 10 min, and then centrifuged at 1,000 x g for 5 min at 37˚C. The lower phase was retained, mixed with chilled Membrane Protein Extraction Buffer B, incubated on ice for 2 min and then at 37˚C for 5 min, and centrifuged again at 1,000 x g for 5 min at 37˚C. After removing the upper liquid, the pelleted membrane proteins were dissolved in chilled Membrane Protein Solubilization Buffer C. Protease Inhibitor D was added to all extraction and solubilization buffers prior to use. Total protein was extracted from cells lysed in RIPA buffer (cat. no. HY-K1001; MedChemExpress) supplemented with a protease inhibitor cocktail (cat. no. K1019; APExBIO Technology LLC). The protein extracts (500 μl) were then incubated with rabbit anti-HMGN2 antibody (dilution, 1:250; cat. no. 10953-1-AP; Proteintech Group, Inc.) or control IgG (dilution, 1:250; cat. no. B30011; Abmart Pharmaceutical Technology Co., Ltd.) at room temperature for 2 h, after which 20 μl protein A/G beads (cat. no. K1305; APExBIO Technology LLC) were added and incubated at room temperature for 1 h. After elution with IP eluent (cat. no. T10007; Abmart Pharmaceutical Technology Co., Ltd.), the antibody-protein complex was resolved via SDS-PAGE and Coomassie blue staining was performed at room temperature for 2 h. The SDS-PAGE gel and beads binding the antibody-protein complex of the membrane protein were processed for protein identification by PTM BIO LLC using in-gel tryptic digestion and liquid chromatography-tandem mass spectrometry (LC-MS/MS) analysis.

For in-gel tryptic digestion, gel slices were destained, reduced with dithiothreitol, alkylated with iodoacetamide, and digested overnight with trypsin (37˚C). Peptides were extracted and dried under a stream of nitrogen gas at 320˚C, and subsequently analyzed by LC-MS/MS. Peptides were separated on a home-made reversed-phase analytical column (15 cm x 75 μm) using an EASY-nLC 1000 UPLC system (Thermo Fisher Scientific, Inc.). The mobile phase consisted of solvent A (0.1% formic acid and 2% acetonitrile in water) and solvent B (0.1% formic acid and 98% acetonitrile in water). The following gradient was applied at a flow rate of 400 nl/min with the column temperature set to 60˚C: 0-16 min, 6-23% B; 16-24 min, 23-35% B; 24-27 min, 35-80% B; 27-30 min, 80% B. The injection volume was 3 μl, corresponding to 1.5 μg of peptides, and no internal standards were employed. MS was performed on a Q Exactive Plus (Thermo Fisher Scientific, Inc.) with a nanospray ionization source in positive ion mode (2.0 kV). Full MS scans (350-1,800 m/z) were acquired at a resolution of 70,000, followed by data-dependent MS/MS scans (NCE 28; resolution, 17,500) of the top 20 ions with dynamic exclusion of 15.0 sec. Automatic gain control was set to 5x10^4. MS/MS data were searched using the MaxQuant search engine (version 1.6.15.0; https://www.maxquant.org/maxquant/) with trypsin/P as enzyme (≤2 missed cleavages). The precursor tolerance was 10 ppm and the fragment tolerance was 0.02 Da. Carbamidomethylation of cysteine was set as a fixed modification, and methionine oxidation was included as a variable modification. Peptide confidence was set to high with an ion score >20.

Immunofluorescence. A total of ~1x10^5 CAL-27 cells were seeded on microscope coverslips in 12-well plates and

cultured at 37˚C. The cells were then washed with 1X PBS, fixed with 4% paraformaldehyde at room temperature for 20 min, permeabilized with 0.01% Triton X-100 and blocked with 5% BSA (cat. no. AWB-6015; Abmart Pharmaceutical Technology Co., Ltd.) at room temperature for 1 h, before they were incubated with primary antibodies against STT3B (dilution, 1:100; cat. no. 15323-1-AP; Proteintech Group, Inc.) or PD-L1 (dilution, 1:100; cat. no. A27937; ABclonal Biotech Co., Ltd.) at 4˚C overnight. Nuclei were stained with DAPI (cat. no. C3362; APExBIO Technology LLC). After being washed three times with 1X PBS, the cells were incubated with an FITC-conjugated secondary antibody (dilution, 1:100; cat. no. AS011; ABclonal Biotech Co., Ltd.) at room temperature for 2 h. The cells were subsequently visualized using a FLUOVIEW FV3000 confocal laser scanning microscope (Olympus Corporation) and images were captured.

Western blot analysis. The downstream validation of the IP/MS results was conducted by western blotting, as outlined subsequently. After incubation with 20 μg/ml His-tagged HMGN2 at 37˚C for 10 and 60 min, proteins were extracted from CAL-27 cells using RIPA buffer (cat. no. HY-K1001; MedChemExpress), which primarily consists of 50 mM Tris (pH 7.4), 150 mM NaCl, 1% Triton X-100, 1% sodium deoxycholate and 0.1% SDS, as well as sodium orthovanadate and EDTA. Protein quantification was performed using the Enhanced BCA Protein Assay Kit (cat. no. P0010S; Beyotime Biotechnology) according to the manufacturer's instructions. The protein extracts were subsequently separated by 10% SDS-PAGE (10 μg per lane), before being transferred to PVDF membranes. The membranes were blocked with 5% fat-free milk at room temperature for 1 h and were subsequently incubated with primary antibodies against HMGN2 (dilution, 1:1,000; cat. no. 10953-1-AP; Proteintech Group, Inc.), STT3B (dilution, 1:1,000; cat. no. 15323-1-AP; Proteintech Group, Inc.), PD-L1 (dilution, 1:1,000; cat. no. A27937; ABclonal Biotech Co., Ltd.), gasdermin D (GSDMD; dilution, 1:1,000; cat. no. ab210070; Abcam), caspase-1 (dilution, 1:1,000; cat. no. 2225; Cell Signaling Technology, Inc.) and GAPDH (dilution, 1:5,000; cat. no. AC002; ABclonal Biotech Co., Ltd.) at 4˚C overnight. The antibodies against caspase-1 and GSDMD were also used to detect their respective cleaved forms (cleaved caspase-1 and GSDMD-N). After being washed, the membranes were incubated at room temperature for 2 h with a horseradish peroxidase-labelled secondary antibody (dilution, 1:5,000; cat. nos. AS014 and AS003; ABclonal Biotech Co., Ltd.). Protein bands were subsequently visualized using an enhanced chemiluminescence reagent (cat. no. WBULS0500; MilliporeSigma; Merck KGaA) and imaged with a ChemiDoc MP Imaging system (Bio-Rad Laboratories, Inc.). Protein expression levels were semi-quantified using ImageJ software (version 1.8.0; National Institutes of Health).

Depletion of STT3B. Antibody-mediated depletion is an established method for selectively eliminating cell populations expressing target proteins, as documented in previous literature (14). Antibody-dependent cell-mediated cytotoxicity is a recognized consideration, with certain therapeutic antibodies, such as PD-L1 inhibitors, demonstrating potent efficacy in cancer treatment through their depletion mechanisms (15). In 2014, our laboratory demonstrated that ~50% of HMGN2 was depleted from the supernatant of FITC-labelled activated $CD8^+$ T cells using an anti-human HMGN2 antibody (5). In addition, the tumour-killing capacity of γδ T cells can be functionally blocked by anti-human HMGN2 antibodies (6). Building upon this methodology, CAL-27 cells incubated with 10 μg/ml anti-STT3B antibody (cat. no. 15323-1-AP; Proteintech Group, Inc.) at 37˚C for 2 h in the present study were designated the 'STT3B-depleted' group.

Fluorescence-labelled HMGN2 transmembrane transport assay with anti-STT3B antibodies. A total of ~$1x10^5$ CAL-27 cells were seeded in 35-mm glass bottom dishes with 10-mm microwells. After being washed with PBS, the cells were divided into three groups: The control, HMGN2 and STT3B-depleted groups. Cells in the depleted group were treated with 10 μg/ml anti-STT3B antibody (cat. no. 15323-1-AP; Proteintech Group, Inc.) at 37˚C for 2 h. Subsequently, 20 μg/ml FITC-labelled HMGN2 was added and the cells were incubated at 37˚C for 10 min. Nuclear staining of CAL-27 cells was performed using Hoechst 33258 (cat. no. A3466; APExBIO Technology LLC) at room temperature for 10 min. Cells not treated with anti-STT3B antibody were used as a positive control (HMGN2 group). The control group was treated with PBS. Imaging was performed using a FLUOVIEW FV3000 confocal laser scanning microscope (Olympus Corporation).

Protein-protein docking between STT3B and HMGN2. The Protein Data Bank (PDB) format and FASTA sequences of the STT3B protein structural domain were downloaded from the PDB database (https://www.rcsb.org/structure/6S7T). The protein structure of HMGN2 was predicted using Swiss-Model (https://swissmodel.expasy.org/) according to the FASTA sequence obtained from the National Center for Biotechnology Information database (https://www.ncbi.nlm.nih.gov/gene/3151).

The rigid protein-protein docking module ZDOCK (version 3.0.2; https://zdock.umassmed.edu/) was used to identify the docking sites between STT3B and HMGN2, and ZDOCK scores were calculated. Using AlphaFold3 (16) (https://www.alphafoldserver.com), the 3D structure of STT3B was simulated with HMGN2. The predictive structures were visualized using Discovery Studio 2019 Client (BIOVIA; Dassault Systèmes S.E.).

Statistical analysis. GraphPad Prism software (version 8.0.1; Dotmatics) was used for all statistical analyses. Experiments were performed in three independent biological replicates. The quantitative data are shown as the mean ± SEM. Comparisons between two groups were performed using unpaired Student's two-tailed t-tests, whereas statistical comparisons among more than two groups were performed by one-way analysis of variance followed by a Bonferroni post hoc correction. $P<0.05$ was considered to indicate a statistically significant difference.

Results

Functional identification of the antitumour activity of the HMGN2 protein in CAL-27 cells. After the cells were incubated with various concentrations of HMGN2 for 24 h, the apoptotic

response of CAL-27 cells was assessed by bright-field microscopy (Fig. 1A). In addition, the HMGN2 protein was incubated with CAL-27 cells at 37˚C for 12 and 24 h, and the cells were subject to flow cytometry. Analysis of flow cytometry results revealed that compared with that in the control group, the relative percentage of CAL-27 cells undergoing late apoptosis was significantly greater following HMGN2 incubation. A total of ~14 and 23% of the CAL-27 cells treated with HMGN2 for 12 and 24 h, respectively, were Annexin V^+ and propidium $iodide^+$ (Fig. 1B and C). This was significantly higher than the values observed in the control group. The present results suggested that HMGN2 induced the apoptosis of CAL-27 cells.

HMGN2 binds to the membrane and is transported into tumour cells. CAL-27 cells were incubated with FITC-labelled HMGN2 for 10 min, 1 and 2 h, and were subsequently detected by confocal laser scanning microscopy. The results revealed that FITC-labelled HMGN2 was localised to the membranes of CAL-27 cells and could be transported into the cells (Fig. 2).

IP/MS indicates that STT3B is a receptor of HMGN2 on CAL-27 cell membranes. The present study performed IP/MS to identify the notable receptors associated with HMGN2. After incubation with HMGN2, the total proteins and membrane proteins of CAL-27 cells were extracted and immunoprecipitated using magnetic beads so that the interacting proteins could be visualized by Coomassie blue staining after SDS-PAGE (Fig. 3A). Membrane proteins were subsequently identified via mass spectrometry.

The results of magnetic bead analysis revealed 842 proteins that were immunoprecipitated by the anti-HMGN2 antibody and 530 proteins identified via SDS-PAGE. The results of magnetic bead analysis revealed 899 proteins that were immunoprecipitated by the anti-IgG antibody and 180 proteins identified via SDS-PAGE. However, only 313 proteins were detected after immunoprecipitation with the anti-HMGN2 antibody and not with anti-IgG according to the results of magnetic bead analysis. Similarly, only 370 proteins exclusive to the anti-HMGN2 antibody were detected via SDS-PAGE. The results from magnetic bead and gel analyses were subsequently combined to obtain the 30 top proteins that interact with HMGN2 (Fig. 3B). Only 6 of the 30 proteins screened were located on the membranes of cells, among which STT3B had the highest protein score and propensity score matching (PSM) value (Table I). Immunofluorescence staining supported the subcellular localization of STT3B on cell membranes (Fig. 3C).

STT3B is an important receptor of HMGN2 on CAL-27 cell membranes. Given that CAL-27 cells respond to HMGN2, the present study examined the interaction effects of HMGN2 and STT3B on total protein and membrane proteins in CAL-27 cells. Immunoprecipitation results indicated that STT3B physically interacted with HMGN2 (Fig. 4A and B). To determine whether STT3B was important for HMGN2 translocation into CAL-27 cells, STT3B was blocked on the membrane using an anti-STT3B antibody, and the results revealed that compared with that of the positive control, which was incubated with the FITC-labelled HMGN2 protein, the level of FITC-labelled HMGN2 protein on the membranes of CAL-27 cells visibly decreased in the presence of the anti-STT3B antibody (Fig. 4C).

The present study also predicted the best position for the interaction between HMGN2 and STT3B using rigid protein-protein docking (Fig. 4D and E). The highest ZDOCK score for an interaction was 1,846.143. Furthermore, simulated HMGN2 formed hydrogen bonds at amino acid sites such as Asn3-Asp103, Asn3-Asn623 and Ala4-Ser404 (Table II). AlphaFold3 simulated the interaction structure of STT3B and HMGN2 in which hydrogen bonds were shown to have formed, including at sites such as Ala7-Asn67, Ala7-Trp677 and Ala6-Ser402. The interface predicted template modeling score and predicted template modeling score were 0.78 and 0.80, respectively (Table III), indicating a good predictive power regarding the aforementioned binding structure. Comprehensive analysis revealed that the proteins HMGN2 and STT3B formed a stable protein docking model.

HMGN2 promotes the nuclear translocation of membrane PD-L1, activating the PD-L1/caspase-1/GSDMD axis. After incubation with HMGN2, the expression of STT3B was upregulated, which further supported the association between STT3B and HMGN2 (Fig. 5A and B). Few studies have examined the function of STT3B in cancer cell death, but STT3B has been shown to mediate the glycosylation of PD-L1, which induces immune evasion (13). PD-L1, an immune checkpoint regulator, shields cancer cells from host immune responses (17). However, PD-L1 can also trigger pyroptosis in cancer cells, indicating that PD-L1 is a signalling mediator that affects tumour outcomes (18). In addition to apoptosis, ferroptosis and necrosis, pyroptosis serves an important role in tumour cell death and is characterized as a GSDM-mediated mode of programmed cell death. In terms of the molecular mechanism of pyroptosis, caspase-1, -4, -5, -11 and -3 have been shown to cleave GSDMD or GSDME to induce pyroptosis (19). The results of the present study revealed that the expression of PD-L1/caspase-1/GSDMD axis components was significantly upregulated in response to HMGN2 stimulation (Fig. 5A and B), while the cleavage ratios of both caspase-1 and GSDMD showed no statistically significant alterations. In addition, treatment with HMGN2 was shown to induce the nuclear translocation of PD-L1 from the membranes of cancer cells (Fig. 5C).

Discussion

HMG proteins constitute an abundant family of non-histone proteins localised in the cell nuclei of vertebrates and invertebrates (5). The HMG protein family comprises three subfamilies: HMGB, HMGA and HMGN, which each perform a distinct nuclear function (11). However, other peptides in the HMG protein family also have important roles. For example, as an abundant, highly conserved cellular protein, HMGB1 is considered a nuclear DNA-binding protein (20). A decade-long search revealed HMGB1 as a late toxic cytokine of endotoxaemia (21-23). Upon release by macrophages in response to endotoxins, HMGB1 triggers the activation of various proinflammatory mediators, which can be fatal to healthy animals (24). Additionally, HMGB1-3 operate as universal sentinel proteins for nucleic acid-mediated innate immune responses (25).

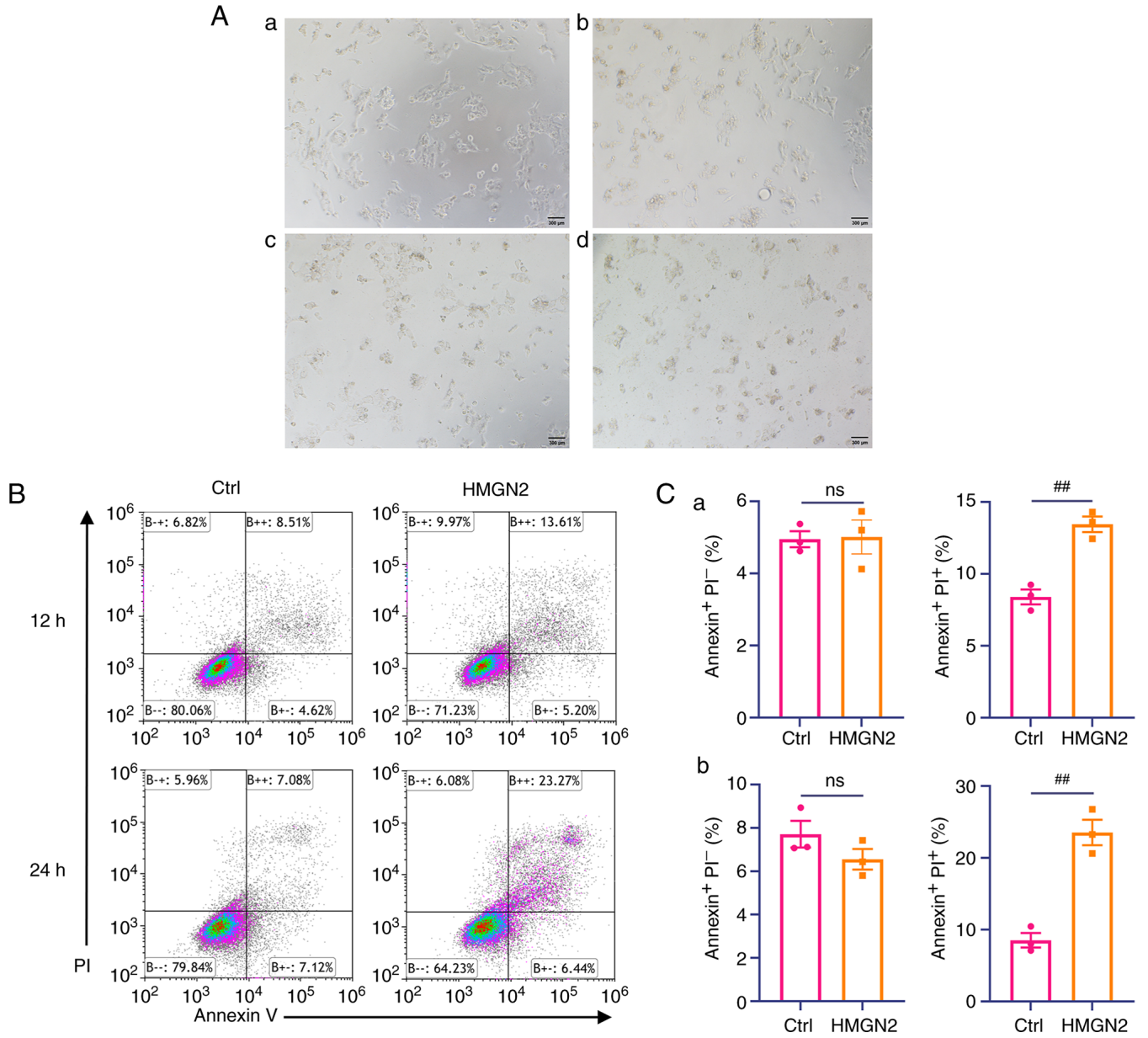

Figure 1. HMGN2 induces apoptosis in CAL-27 cells. (A) CAL-27 cells were observed under a bright-field microscope after 24 h of incubation with (Aa) 0, (Ab) 5, (Ac) 10 or (A-d) 20 μg/ml HMGN2. (B) Representative flow cytometry plots showing apoptosis of CAL-27 cells following incubation with 20 μg/ml HMGN2. (C) Relative percentage of apoptotic CAL-27 cells treated with HMGN2 for (Ca) 12 and (Cb) 24 h. The control group was treated with PBS. Annexin$^+$ PI$^-$ represents cells in the early phase of apoptosis and Annexin$^+$ PI$^+$ represents cells in the last phase of apoptosis. Scale bar, 300 μm. Data are presented as the mean ± SEM (n=3). $^{\#\#}$P<0.01 vs. control. Ctrl, control; HMGN2, high-mobility group nucleosomal-binding domain 2; ns, not significant; PI, propidium iodide.

HMGA proteins modulate the transcription of a number of genes through interactions with transcription factors and altering the structure of chromatin. HMGA proteins have been shown to be involved in both benign and malignant neoplasia via numerous pathways. A number of benign human mesenchymal tumours show HMGA gene rearrangements. Conversely, malignant tumours exhibit wild-type HMGA protein upregulation, which is frequently a cause of neoplastic cell transformation (26,27).

The HMGN family comprises five chromatin architectural proteins present in higher vertebrates (28). HMGN5, located on human chromosome Xq13.3, is a prominent member of the HMGN family, and exhibits a functional nucleotide-binding domain and a negatively charged C-terminus (28). The HMGN5 protein can rapidly translocate into the nucleus and interact with nucleosomes, thereby affecting transcription (29). Previous studies have indicated that the expression of the HMGN5 gene is upregulated in numerous human tumours and that HMGN5 is activated in tumour models (30,31).

HMGN2 is one of the most abundant non-histone nuclear proteins in both vertebrates and invertebrates, which participates in chromatin remodelling and transcriptional activation (1-4). Additionally, HMGN2 is associated with the recognition of various types of tumour cells (32-34), antineoplastic activity (5,35,36) and the prediction of various tumours (37-40). Previous studies have demonstrated that HMGN2 expressed by CD8$^+$ T cells has strong antitumour

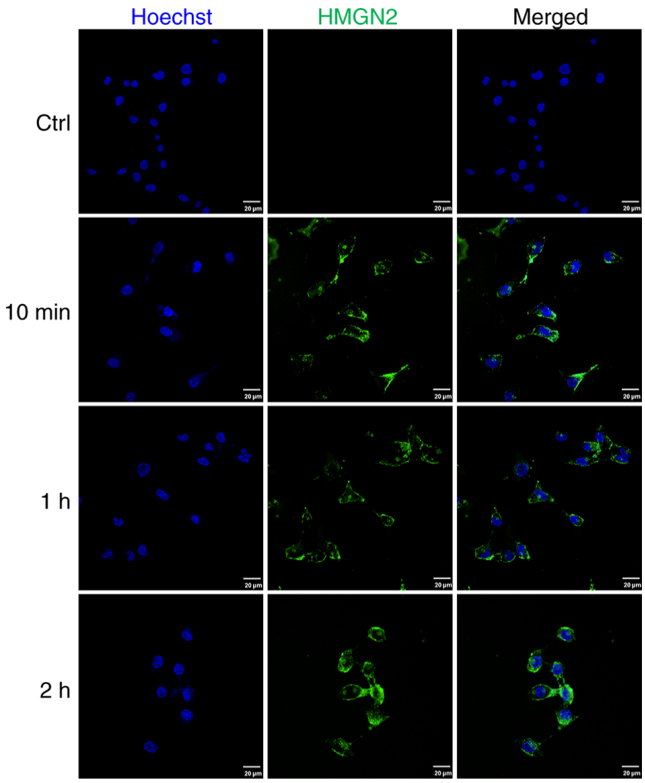

Figure 2. Microscopic imaging of CAL-27 cells after incubation with FITC-labelled HMGN2. HMGN2 was translocated into CAL-27 cells through binding to the cell membrane after incubation with 20 μg/ml FITC-labelled HMGN2 for 10 min, 1 or 2 h. Scale bar, 20 μm. Ctrl, control; HMGN2, high-mobility group nucleosomal-binding domain 2.

effects through rapid recognition and transport into tumour cells (5,41). For example, a study performed by Li *et al* (42) demonstrated that T cells engineered to express HMGN2, designated 'HMGN2-T cells', effectively kill cancer cells and enhance the secretion of IL-2 and TNF-α. Similarly, Su *et al* (5) showed that HMGN2 released by $CD8^+$ T cells can enter tumour cells and induce cell death. However, the specific mechanism by which HMGN2 affects tumour cells remains to be fully elucidated, raising the important question of how HMGN2 identifies and interacts with tumour cells. The present study aimed to detect receptors of HMGN2 on tumour cell membranes and to elucidate the mechanism through which HMGN2 molecule induces tumour cell apoptosis.

To provide evidence of the antitumour effect of HMGN2, the present study first incubated CAL-27 cells with HMGN2 and assessed their degree of apoptosis via flow cytometry. Given the precise location of FITC-labelled HMGN2 on the membranes of CAL-27 cells, the present study hypothesized that the presence of a specific receptor on the cell membrane was responsible for mediating signal communication between HMGN2 and CAL-27 cells, leading to tumour cell death. In the present study, six proteins were identified to be localized to the cytoplasmic membrane through qualitative screening via IP/MS, in which STT3B emerged as the preferred protein, exhibiting the highest protein score, unique peptide count and PSM value.

The immunoprecipitation results verified the interaction between HMGN2 and STT3B; however, the evidence was not significant enough to establish the notable role of STT3B in the communication between HMGN2 and CAL-27 cells. To further validate the importance of STT3B, the present study blocked the STT3B protein on the membranes of CAL-27 cells with an anti-STT3B antibody. The resulting findings underscored the importance of STT3B in the interaction between HMGN2 and CAL-27 cells. Additionally, the present study predicted binding conformations and binding sites of HMGN2 to STT3B using ZDOCK and AlphaFold3. Both models revealed numerous hydrogen bond interactions, including Thr5-Trp604, Thr5-Asp606, Ala4-Ser404, Asn3-Asn623 and Asn3-Asp103, indicating that HMGN2 interacted with CAL-27 cells by binding to the membrane protein STT3B. However, the predicted binding residues for the HMGN2-STT3B interaction, as generated by ZDOCK and AlphaFold3, require further validation through site-directed mutagenesis studies.

Research has shown that upregulation of the STT3 isoforms STT3A and STT3B during EMT acts as a key mediator of tumour immune evasion by promoting PD-L1 glycosylation and stabilization (13). In the present study, the expression levels of STT3B and PD-L1 were found to be upregulated following incubation with HMGN2, which was consistent with the findings of the previous study; these results suggested that the upregulation of STT3B expression stimulated by HMGN2 resulted in the glycosylation and stabilization of PD-L1, thus leading to tumour cell death. This observation conflicted with the notion that stabilization of PD-L1 by STT3B promotes immune evasion (43,44). However, this discrepancy can be addressed by considering STT3B/PD-L1 as a dual-function signalling mediator that may simultaneously trigger pyroptosis while also facilitating immune evasion (17,45). Notably, the precise mechanism governing this dual STT3B/PD-L1 functionality remains to be elucidated, thereby constraining a more comprehensive understanding of the multifaceted roles of PD-L1 in tumour biology.

Pyroptosis is defined as a GSDM-mediated form of programmed necrosis (46,47). Numerous studies have established that caspase-1-mediated pyroptosis serves as an important innate immune defence mechanism (46-49). Notably, GSDMD has been identified as a key substrate of both inflammatory caspases, such as caspase-1, and non-canonical caspases, such as caspase-4, -5 and -11, and is considered the primary executor of pyroptotic cell death (49-51). A previous *in vitro* study revealed that GSDMD cleavage is increased in CTLs and contributes to the antitumour function of $CD8^+$ T cells, indicating that GSDMD is important for the ability of CTLs to kill tumour cells (52). Therefore, the present study hypothesized that GSDMD may have been involved in HMGN2-induced tumour cell death. The findings of the present study revealed that HMGN2 upregulated the expression of caspase-1/GSDMD pathway components, revealing an underlying signalling pathway through which HMGN2 may have induced tumour cell death via activation of the canonical pyroptosis pathway. HMGN2 upregulated caspase-1 and GSDMD protein levels but did not significantly alter their cleavage ratios. This 'priming' phenotype is not uncommonly observed in immune-related cell death pathways, suggesting a priming mechanism in which protein accumulation precedes proteolytic activation (53,54). Additionally, PD-L1 was translocated from the plasma membrane to the nucleus; this translocation has been previously reported to mediate GSDMC expression and caspase-8 activation, leading to pyroptosis of tumour cells (18). However, the regulatory effect of PD-L1 on

Table I. Screened proteins identified by mass spectrometry.

Gene name	Molecular weight, kDa	Protein score	Unique peptides	Propensity score matching	Subcellular localization
STT3B	93.6	94	3	3	Plasma membrane
SSR3	21.1	66	3	1	Plasma membrane
ERMP1	100.2	41	2	2	Plasma membrane
TMEM41B	32.5	39	1	1	Plasma membrane
MMP14	65.9	33	1	1	Plasma membrane
STX5	39.6	25	1	1	Plasma membrane

STT3B, oligosaccharyltransferase subunit STT3; SSR3, signal sequence receptor subunit 3; ERMP1, endoplasmic reticulum metallopeptidase 1; TMEM41B, transmembrane protein 41B; STX5, syntaxin-5.

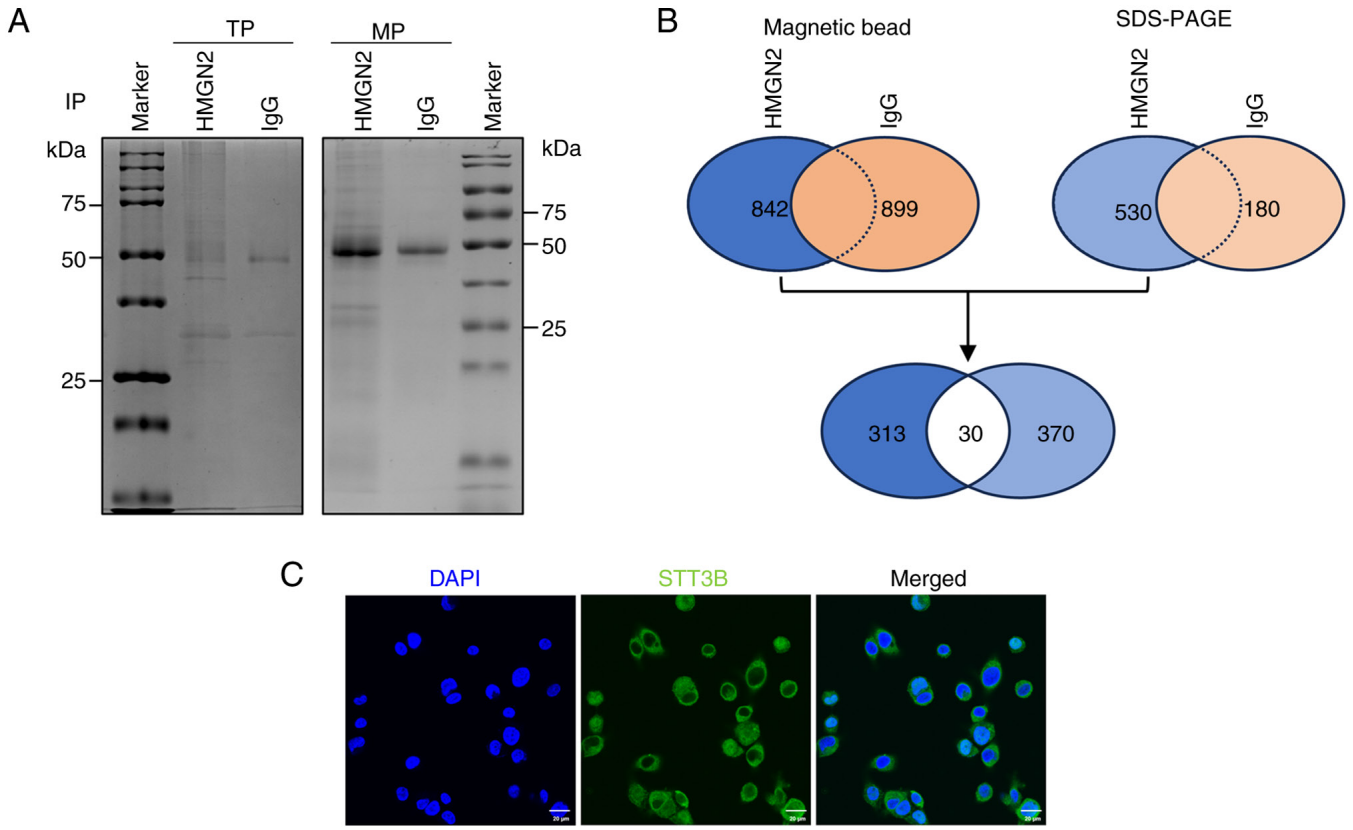

Figure 3. Predicted receptors of HMGN2 determined by IP/MS. (A) IP/MS analysis of HMGN2-associated proteins. The bead-peptide eluate was resolved by SDS-PAGE and Coomassie blue staining. (B) Numbers of proteins identified via IP/MS from magnetic bead-bound antibody-protein complexes and via SDS-PAGE gel separation. (C) Subcellular localization of STT3B in CAL-27 cells. Scale bar, 10 μm. IP, immunoprecipitation; MS, mass spectrometry; TP, total protein; MP, membrane protein; HMGN2, high-mobility group nucleosomal-binding domain 2; STT3B, oligosaccharyltransferase subunit STT3B.

the GSDM family remains to be fully elucidated. Further questions arise regarding how HMGN2 activated STT3B expression and whether HMGN2 influenced the gene expression of the GSDM family. Given that HMGN2 has been confirmed to regulate the activity of transcriptional regulatory factors (1,4) and chromatin (2,3), additional studies are required to elucidate its precise role in these processes.

There are several limitations of the present study that merit consideration. Primarily, while the observed upregulation of GSDMD, a key mediator of pyroptosis, resulted in the conclusion that observed cell death was consistent with pyroptotic processes, direct visualization of characteristic morphological features through live-cell imaging, such as membrane pore formation, cell swelling or large bubble formation, is required to provide additional evidence of this.

Additionally, although the present investigation built upon existing literature and focused primarily on the role of HMGN2 in promoting pyroptosis, the mechanistic basis by which PD-L1 may have concurrently mediated pyroptosis and immune escape has not been fully explored. To improve understanding of this dual functionality, future studies involving STT3B and PD-L1 knockdown or neutralization, combined with detailed analysis of downstream signalling events, would be highly informative.

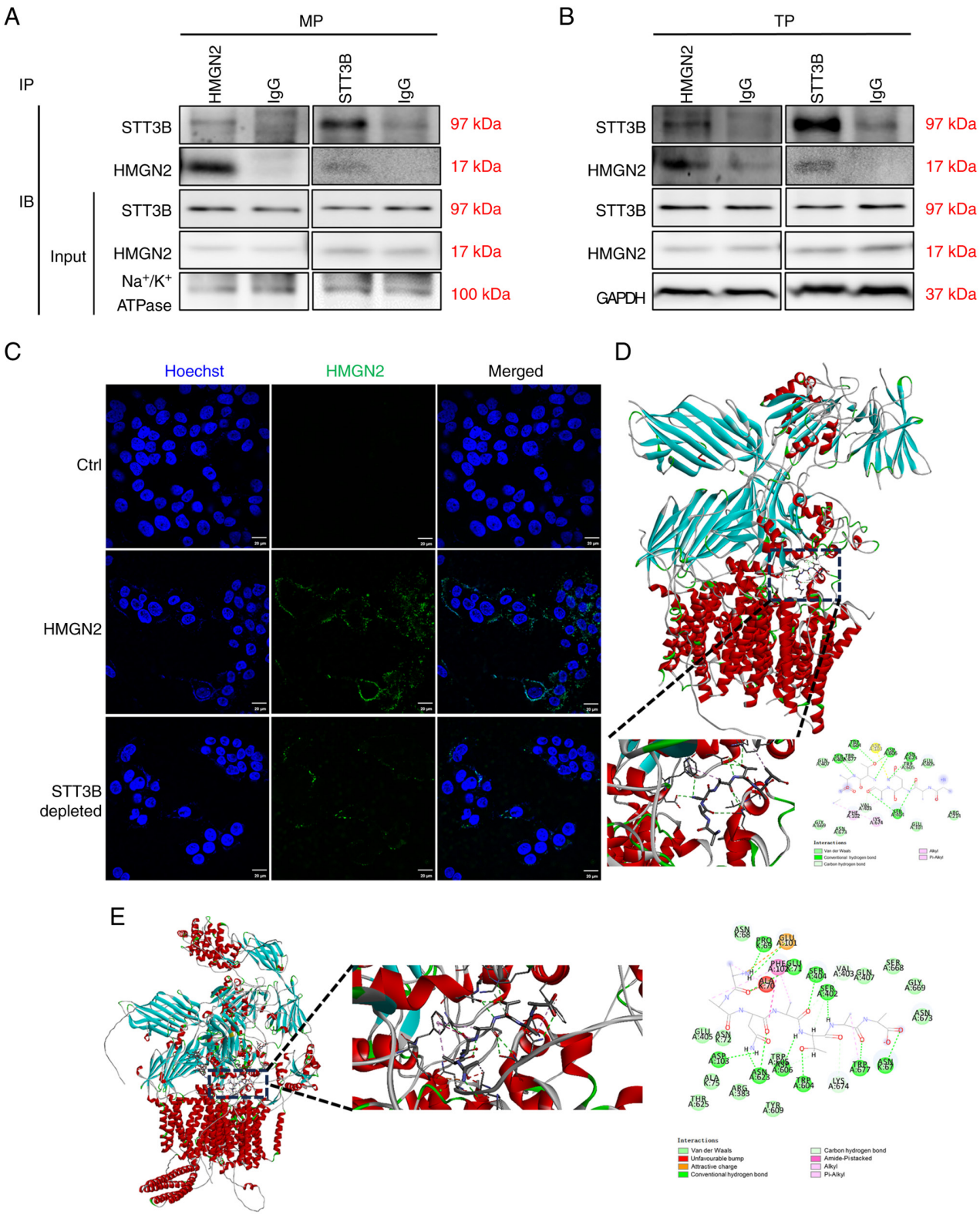

Figure 4. STT3B is an important receptor of HMGN2 on CAL-27 cell membranes. (A and B) CAL-27 cells were incubated with 20 μg/ml HMGN2 (experimental group) or with PBS (control group). Co-IP was carried out using anti-HMGN2 or anti-STT3B antibodies against (A) MP and (B) TP. Immunocomplexes were subsequently detected by IB using anti-STT3B or anti-HMGN2 antibodies. (C) CAL-27 cells were observed under a fluorescence microscope after depletion of STT3B using 10 μg/ml anti-STT3B antibody. Scale bar, 20 μm. (D) Rigid protein-protein docking prediction for the interaction between STT3B and HMGN2. (E) Interaction structure of STT3B and HMGN2 simulated in AlphaFold3. Ctrl, control; IB, immunoblotting; IP, immunoprecipitation; TP, total protein; MP, membrane protein; STT3B, oligosaccharyltransferase subunit STT3B; HMGN2, high-mobility group nucleosomal-binding domain 2.

Furthermore, while the findings of the present study demonstrated coordinated protein-level changes along the STT3B/PD-L1/caspase-1/GSDMD axis, the precise sequence of events and causal relationships within this signalling cascade remain to be fully established. Further studies employing specific inhibitors or systematic loss-of-function approaches

Table II. Analysis of ZDOCK results.

Receptor	Ligand	ZDOCK score	Hydrogen bond interaction	Hydrophobic interaction
STT3B	HMGN2	1,846.143	Asn3-Asp103; Asn3-Asn623; Ala2-Ser404; Ala4-Ser404; Thr5-Trp604; Thr5-Asp606	Ala4-Phe102; Ala7-Lys674

STT3B, oligosaccharyltransferase subunit STT3B; HMGN2, high-mobility group nucleosomal-binding domain 2.

Table III. Analysis of AlphaFold3 results.

Receptor	Ligand	ipTM score	pTM score	Hydrogen bond interaction	Hydrophobic interaction
STT3B	HMGN2	0.78	0.80	Ala7-Asn67; Ala7-Trp677; Ala6-Ser402; Thr5-Trp604; Thr5-Asp606; Ala4-Ser404; Asn3-Asn623; Asn3-Asp103; Asn3-Asn623; Ala1-Pro69; Ala1-Glu71	Ala6-Trp677; Ala4-Phe102; Asn3-Phe102; Ala2-Phe102

STT3B, oligosaccharyltransferase subunit STT3B; HMGN2, high-mobility group nucleosomal-binding domain 2; ipTM, interface predicted template modeling; pTM, predicted template modeling.

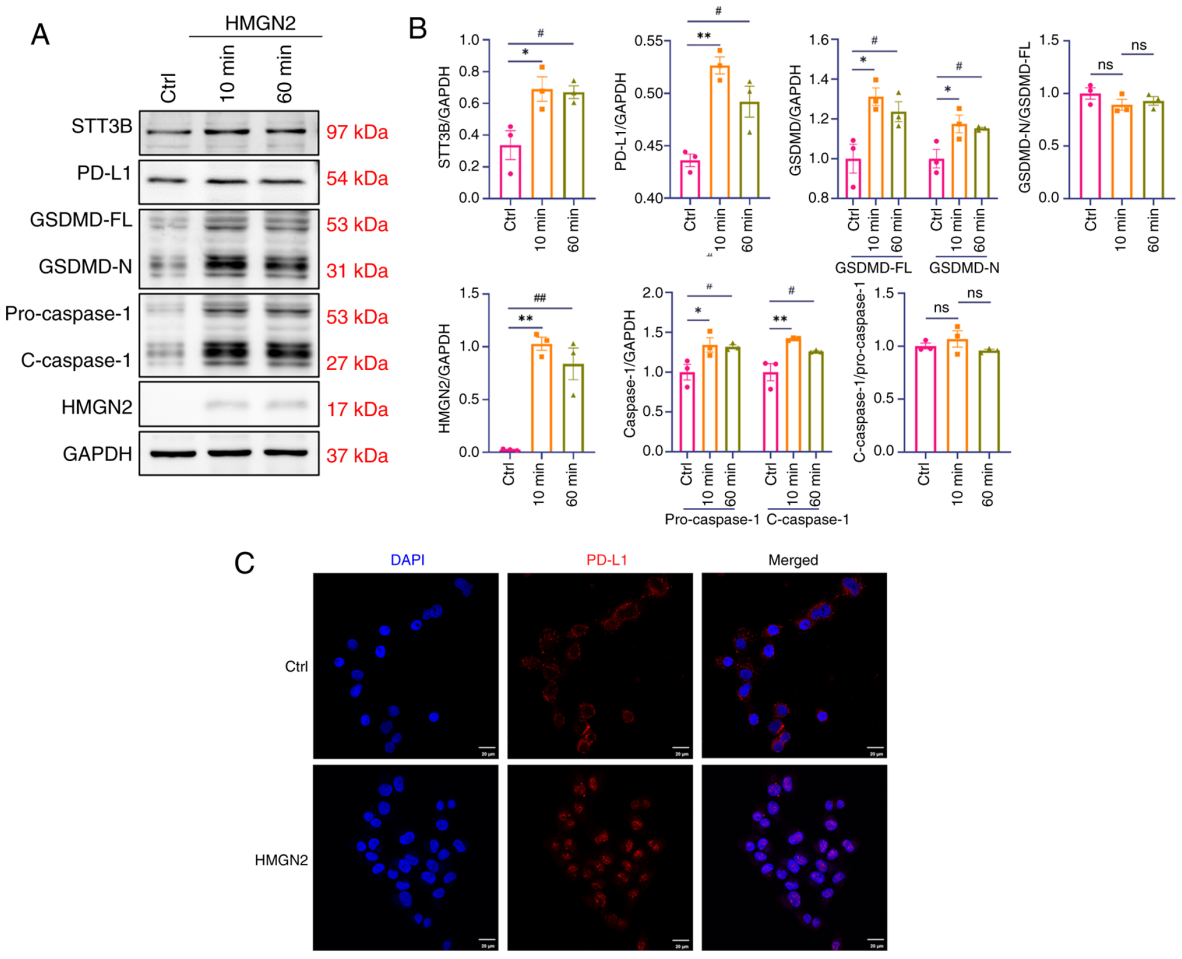

Figure 5. HMGN2 induces pyroptosis in CAL-27 cells through the PD-L1/caspase-1/GSDMD axis. (A) Representative western blot analysis of the PD-L1/caspase-1/GSDMD axis, and the HMGN2 and STT3B proteins in CAL-27 cells after incubation with 20 μg/ml HMGN2 for 10 or 60 min. The Ctrl group was treated with PBS. (B) Semi-quantitative analyses of the PD-L1/caspase-1/GSDMD axis, and the HMGN2 and STT3B proteins in CAL-27 cells (n=3). (C) Representative images showing PD-L1 translocation in CAL-27 cells treated with HMGN2. The Ctrl group was treated with PBS. Scale bar, 20 μm. Data are presented as the mean ± SEM. *P<0.05 and **P<0.01; $^{\#}$P<0.05 and $^{\#\#}$P<0.01. Ctrl, control; ns, not significant; HMGN2, high-mobility group nucleosomal-binding domain 2; PD-L1, programmed cell death 1 ligand 1; GSDMD-N, N-terminal domain of gasdermin D; GSDMD-FL, full-length gasdermin D; STT3B, oligosaccharyltransferase subunit STT3B; C-caspase-1, cleaved caspase-1.

may help to clarify the regulatory hierarchy of this pathway and establish mechanistic causality.

From a methodological standpoint, the antibody-based STT3B depletion approach employed in the present study was based on established protocols and the present specific experimental context. Nevertheless, the use of genetic perturbation methods, such as CRISPR/Cas9 or stable RNA interference, in future work could offer more definitive mechanistic insights.

Finally, all experimental findings in the present study are based on the CAL-27 tongue squamous cell carcinoma model. Further validation across a broader range of cancer models, including additional squamous cell carcinoma subtypes and non-squamous malignancies, would help to assess the generalizability of the proposed mechanism. In addition, *in vivo* studies using immunocompetent mouse models would be valuable to validate the physiological relevance of this pathway and to more comprehensively evaluate the therapeutic potential of HMGN2 within an intact tumour microenvironment.

In conclusion, extracellular HMGN2 may induce pyroptosis in tumour cells through the STT3B/PD-L1/caspase-1/GSDMD axis, indicating the capacity of HMGN2 in antitumour immunotherapy, as well as a new mechanism through which CTLs induce antitumour effects.

Acknowledgements

Not applicable.

Funding

The present work was supported by the Natural Science Foundation of Sichuan Province (grant no. 2022YFS0118) and the Interdisciplinary Research Project of the State Key Laboratory of Oral Diseases (grant no. 2022KXK0402).

Availability of data and materials

The data generated in the present study may be requested from the corresponding author.

Authors' contributions

WH was responsible for the conceptualization and methodology of the present study, as well as contributing to the investigation, formal analysis and composition of the original draft. HC, BC and JC contributed towards the formal analysis of the present study. PZ contributed towards the conceptualization, funding acquisition, and reviewing and editing the manuscript. YF was responsible for conceptualization of the study, as well as reviewing and editing the manuscript. WH and YF confirm the authenticity of all the raw data. All authors read and approved the final manuscript.

Ethics approval and consent to participate

Not applicable.

Patient consent for publication

Not applicable.

Competing interests

The authors declare that they have no competing interests.

References

1. Craig JM, Turner TH, Harrell JC and Clevenger CV: Prolactin drives a dynamic STAT5A/HDAC6/HMGN2 Cis-regulatory landscape exploitable in ER+ breast cancer. Endocrinology 162: bqab036, 2021.
2. He B, Zhu I, Postnikov Y, Furusawa T, Jenkins L, Nanduri R, Bustin M and Landsman D: Multiple epigenetic factors co-localize with HMGN proteins in A-compartment chromatin. Epigenetics Chromatin 15: 23, 2022.
3. Zhang S, Postnikov Y, Lobanov A, Furusawa T, Deng T and Bustin M: H3K27ac nucleosomes facilitate HMGN localization at regulatory sites to modulate chromatin binding of transcription factors. Commun Biol 5: 159, 2022.
4. Eliason S, Su D, Pinho F, Sun Z, Zhang Z, Li X, Sweat M, Venugopalan SR, He B, Bustin M and Amendt BA: HMGN2 represses gene transcription via interaction with transcription factors Lef-1 and Pitx2 during amelogenesis. J Biol Chem 298: 102295, 2022.
5. Su L, Hu A, Luo Y, Zhou W, Zhang P and Feng Y: HMGN2, a new anti-tumor effector molecule of $CD8^+$ T cells. Mol Cancer 13: 178, 2014.
6. Chen J, Fan Y, Cui B, Li X, Yu Y, Du Y, Chen Q, Feng Y and Zhang P: HMGN2: An antitumor effector molecule of γδT cells. J Immunother 41: 118-124, 2018.
7. Xia A, Zhang Y, Xu J, Yin T and Lu XJ: T cell dysfunction in cancer immunity and immunotherapy. Front Immunol 10: 1719, 2019.
8. Mahaki H, Ravari H, Kazemzadeh G, Lotfian E, Daddost RA, Avan A, Manoochehri H, Sheykhhasan M, Mahmoudian RA and Tanzadehpanah H: Pro-inflammatory responses after peptide-based cancer immunotherapy. Heliyon 10: e32249, 2024.
9. Najafi M, Farhood B and Mortezaee K: Contribution of regulatory T cells to cancer: A review. J Cell Physiol 234: 7983-7993, 2019.
10. Li Q, Chen J, Li X, Cui B, Fan Y, Geng N, Chen Q, Zhang P and Feng Y: Increased expression of high-mobility group nucleosomal-binding domain 2 protein in various tumor cell lines. Oncol Lett 15: 4517-4522, 2018.
11. Fan B, Shi S, Shen X, Yang X, Liu N, Wu G, Guo X and Huang N: Effect of HMGN2 on proliferation and apoptosis of MCF-7 breast cancer cells. Oncol Lett 17: 1160-1166, 2019.
12. Breitling J and Aebi M: N-linked protein glycosylation in the endoplasmic reticulum. Cold Spring Harb Perspect Biol 5: a013359, 2013.
13. Hsu JM, Xia W, Hsu YH, Chan LC, Yu WH, Cha JH, Chen CT, Liao HW, Kuo CW, Khoo KH, *et al*: STT3-dependent PD-L1 accumulation on cancer stem cells promotes immune evasion. Nat Commun 9: 1908, 2018.
14. Sutton MS, Bucsan AN, Lehman CC, Kamath M, Pokkali S, Magnani DM, Seder R, Darrah PA and Roederer M: Antibody-mediated depletion of select leukocyte subsets in blood and tissue of nonhuman primates. Front Immunol 15: 1359679, 2024.
15. Chen Z, Kankala RK, Yang Z, Li W, Xie S, Li H, Chen AZ and Zou L: Antibody-based drug delivery systems for cancer therapy: Mechanisms, challenges, and prospects. Theranostics 12: 3719-3746, 2022.
16. Abramson J, Adler J, Dunger J, Evans R, Green T, Pritzel A, Ronneberger O, Willmore L, Ballard AJ, Bambrick J, *et al*: Accurate structure prediction of biomolecular interactions with AlphaFold 3. Nature 630: 493-500, 2024.
17. Xiong W, Gao Y, Wei W and Zhang J: Extracellular and nuclear PD-L1 in modulating cancer immunotherapy. Trends Cancer 7: 837-846, 2021.
18. Hou J, Zhao R, Xia W, Chang CW, You Y, Hsu JM, Nie L, Chen Y, Wang YC, Liu C, *et al*: PD-L1-mediated gasdermin C expression switches apoptosis to pyroptosis in cancer cells and facilitates tumour necrosis. Nat Cell Biol 22: 1264-1275, 2020.
19. Liu W, Peng J, Xiao M, Cai Y, Peng B, Zhang W, Li J, Kang F, Hong Q, Liang Q, *et al*: The implication of pyroptosis in cancer immunology: Current advances and prospects. Genes Dis 10: 2339-2350, 2022.

20. Yang Z, Simovic MO, Edsall PR, Liu B, Cancio TS, Batchinsky AI, Cancio LC and Li Y: HMGB1 inhibition to ameliorate organ failure and increase survival in trauma. Biomolecules 12: 101, 2022.
21. Tang D, Kang R, Xiao W, Zhang H, Lotze MT, Wang H and Xiao X: Quercetin prevents LPS-induced high-mobility group box 1 release and proinflammatory function. Am J Respir Cell Mol Biol 41: 651-660, 2009.
22. Tang Y, Lv B, Wang H, Xiao X and Zuo X: PACAP inhibit the release and cytokine activity of HMGB1 and improve the survival during lethal endotoxemia. Int Immunopharmacol 8: 1646-1651, 2008.
23. Czura CJ, Wang H and Tracey KJ: Dual roles for HMGB1: DNA binding and cytokine. J Endotoxin Res 7: 315-321, 2001.
24. Wang S and Zhang Y: HMGB1 in inflammation and cancer. J Hematol Oncol 13: 116, 2020.
25. Yanai H, Ban T, Wang Z, Choi MK, Kawamura T, Negishi H, Nakasato M, Lu Y, Hangai S, Koshiba R, *et al*: HMGB proteins function as universal sentinels for nucleic-acid-mediated innate immune responses. Nature 462: 99-103, 2009.
26. De Martino M, Fusco A and Esposito F: HMGA and cancer: A review on patent literatures. Recent Pat Anticancer Drug Discov 14: 258-267, 2019.
27. Meireles Da Costa N, Ribeiro Pinto LF, Nasciutti LE and Palumbo A Jr: The prominent role of HMGA proteins in the early management of gastrointestinal cancers. Biomed Res Int 2019: 2059516, 2019.
28. Nanduri R, Furusawa T and Bustin M: Biological functions of HMGN chromosomal proteins. Int J Mol Sci 21: 449, 2020.
29. Rochman M, Postnikov Y, Correll S, Malicet C, Wincovitch S, Karpova TS, McNally JG, Wu X, Bubunenko NA, Grigoryev S and Bustin M: The interaction of NSBP1/HMGN5 with nucleosomes in euchromatin counteracts linker histone-mediated chromatin compaction and modulates transcription. Mol Cell 35: 642-656, 2009.
30. Mou J, Huang M, Wang F, Xu X, Xie H, Lu H, Li M, Li Y, Kong W and Chen J: HMGN5 escorts oncogenic STAT3 signaling by regulating the chromatin landscape in breast cancer tumorigenesis. Mol Cancer Res 20: 1724-1738, 2022.
31. Yao K, He L, Gan Y, Liu J, Tang J, Long Z and Tan J: HMGN5 promotes IL-6-induced epithelial-mesenchymal transition of bladder cancer by interacting with Hsp27. Aging (Albany NY) 12: 7282-7298, 2020.
32. He B, Deng T, Zhu I, Furusawa T, Zhang S, Tang W, Postnikov Y, Ambs S, Li CC, Livak F, *et al*: Binding of HMGN proteins to cell specific enhancers stabilizes cell identity. Nat Commun 9: 5240, 2018.
33. Nanduri R, Furusawa T, Lobanov A, He B, Xie C, Dadkhah K, Kelly MC, Gavrilova O, Gonzalez FJ and Bustin M: Epigenetic regulation of white adipose tissue plasticity and energy metabolism by nucleosome binding HMGN proteins. Nat Commun 13: 7303, 2022.
34. Morande PE, Borge M, Abreu C, Galletti J, Zanetti SR, Nannini P, Bezares RF, Pantano S, Dighiero G, Oppezzo P, *et al*: Surface localization of high-mobility group nucleosome-binding protein 2 on leukemic B cells from patients with chronic lymphocytic leukemia is related to secondary autoimmune hemolytic anemia. Leuk Lymphoma 56: 1115-1122, 2015.
35. Wu Z, Huang Y, Yuan W, Wu X, Shi H, Lu M and Xu A: Expression, tumor immune infiltration, and prognostic impact of HMGs in gastric cancer. Front Oncol 12: 1056917, 2022.
36. Liang G, Xu E, Yang C, Zhang C, Sheng X and Zhou X: Nucleosome-binding protein HMGN2 exhibits antitumor activity in human SaO2 and U2-OS osteosarcoma cell lines. Oncol Rep 33: 1300-1306, 2015.
37. Lin J, Cai Y, Wang Z, Ma Y, Pan J, Liu Y and Zhao Z: Novel biomarkers predict prognosis and drug-induced neuroendocrine differentiation in patients with prostate cancer. Front Endocrinol (Lausanne) 13: 1005916, 2023.
38. Bin-Alee F, Arayataweegool A, Buranapraditkun S, Mahattanasakul P, Tangjaturonrasme N, Hirankarn N, Mutirangura A and Kitkumthorn N: Transcriptomic analysis of peripheral blood mononuclear cells in head and neck squamous cell carcinoma patients. Oral Diseases 27: 1394-1402, 2021.
39. Yu B, Geng C, Wu Z, Zhang Z, Zhang A, Yang Z, Huang J, Xiong Y, Yang H and Chen Z: A CIC-related-epigenetic factors-based model associated with prediction, the tumor microenvironment and drug sensitivity in osteosarcoma. Sci Rep 14: 1308, 2024.
40. Antony F, Deantonio C, Cotella D, Soluri MF, Tarasiuk O, Raspagliesi F, Adorni F, Piazza S, Ciani Y, Santoro C, *et al*: High-throughput assessment of the antibody profile in ovarian cancer ascitic fluids. Oncoimmunology 8: e1614856, 2019.
41. Hu A, Dong X, Liu X, Zhang P, Zhang Y, Su N, Chen Q and Feng Y: Nucleosome-binding protein HMGN2 exhibits anti-tumor activity in oral squamous cell carcinoma. Oncol Lett 7: 115-120, 2014.
42. Li H, Wu X, Bu D, Wang L, Xu X, Wang Y, Liu Y and Zhu P: Recombinant jurkat cells (HMGN2-T cells) secrete cytokines and inhibit the growth of tumor cells. J Mol Histol 53: 741-751, 2022.
43. Sun Z, Ma X, Zhao C, Fan L, Yin S and Hu H: Delta-tocotrienol disrupts PD-L1 glycosylation and reverses PD-L1-mediated immune suppression. Biomed Pharmacother 170: 116078, 2024.
44. Xu S, Wang H, Zhu Y, Han Y, Liu L, Zhang X, Hu J, Zhang W, Duan S, Deng J, *et al*: Stabilization of EREG via STT3B-mediated N-glycosylation is critical for PDL1 upregulation and immune evasion in head and neck squamous cell carcinoma. Int J Oral Sci 16: 47, 2024.
45. Blasco MT and Gomis RR: PD-L1 controls cancer pyroptosis. Nat Cell Biol 22: 1157-1159, 2020.
46. Anderson MJ, den Hartigh AB and Fink SL: Molecular mechanisms of pyroptosis. Methods Mol Biol 2641: 1-16, 2023.
47. Shi J, Gao W and Shao F: Pyroptosis: Gasdermin-mediated programmed necrotic cell death. Trends Biochem Sci 42: 245-254, 2017.
48. Li Y and Jiang Q: Uncoupled pyroptosis and IL-1β secretion downstream of inflammasome signaling. Front Immunol 14: 1128358, 2023.
49. Zuo Y, Chen L, Gu H, He X, Ye Z, Wang Z, Shao Q and Xue C: GSDMD-mediated pyroptosis: A critical mechanism of diabetic nephropathy. Expert Rev Mol Med 23: e23, 2021.
50. Huang Y, Wang S, Huang F, Zhang Q, Qin B, Liao L, Wang M, Wan H, Yan W, Chen D, *et al*: c-FLIP regulates pyroptosis in retinal neurons following oxygen-glucose deprivation/recovery via a GSDMD-mediated pathway. Ann Anat 235: 151672, 2021.
51. Chen Y, Long T, Chen J, Wei H, Meng J, Kang M, Wang J, Zhang X, Xu Q, Zhang C and Xiong K: WTAP participates in neuronal damage by protein translation of NLRP3 in an m6A-YTHDF1-dependent manner after traumatic brain injury. Int J Surg 110: 5396-5408, 2024.
52. Xi G, Gao J, Wan B, Zhan P, Xu W, Lv T and Song Y: GSDMD is required for effector CD8+ T cell responses to lung cancer cells. Int Immunopharmacol 74: 105713, 2019.
53. Yan H, Luo B, Wu X, Guan F, Yu X, Zhao L, Ke X, Wu J and Yuan J: Cisplatin induces pyroptosis via activation of MEG3/NLRP3/caspase-1/GSDMD pathway in Triple-negative breast cancer. Int J Biol Sci 17: 2606-2621, 2021.
54. Liu Y, Fang Y, Chen X, Wang Z, Liang X, Zhang T, Liu M, Zhou N, Lv J, Tang K, *et al*: Gasdermin E-mediated target cell pyroptosis by CAR T cells triggers cytokine release syndrome. Sci Immunol 5: eaax7969, 2020.